Expanded View Figures

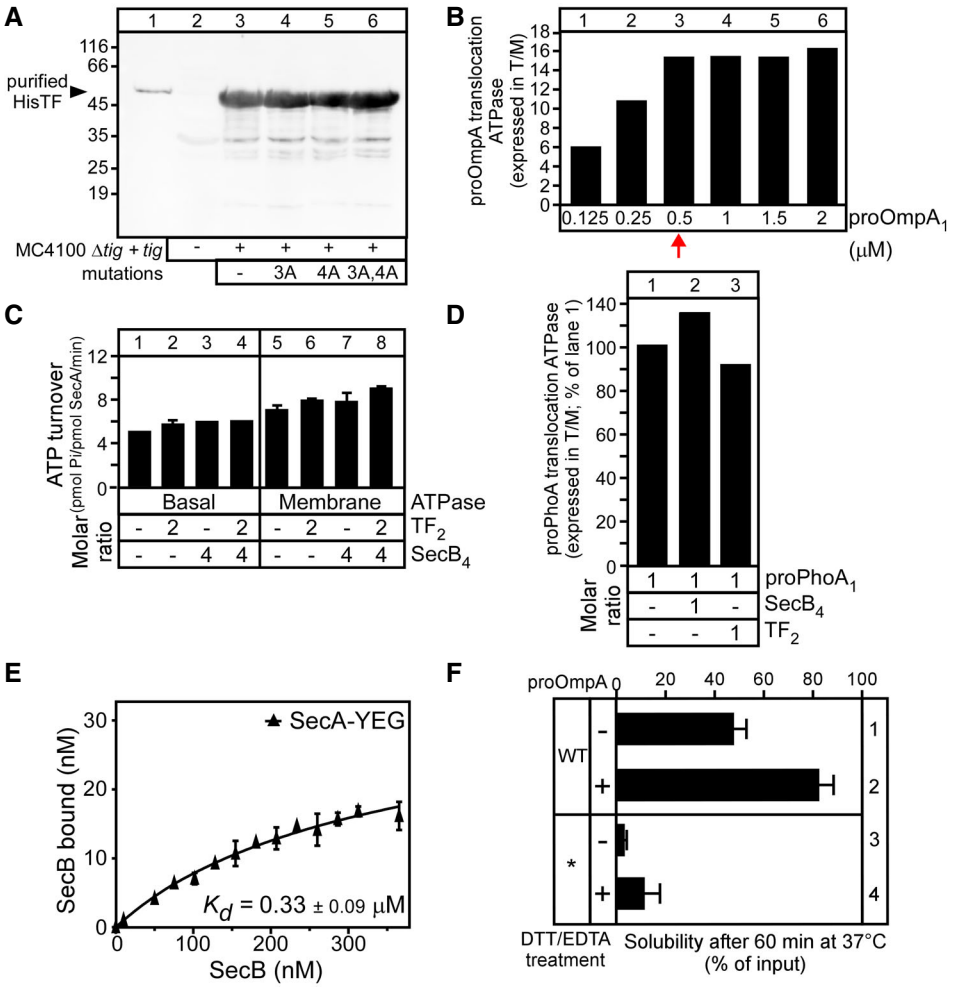

Figure EV1. TF intracellular levels, pro-OmpA-induced translocation ATPase assay and SecB affinity of SecA-YEG IMVs (related to Figs 1, 2 and 4).

A Intracellular levels of TF or derivatives in MC4100Δ*secB*Δ*tig*cells carrying pASK IBA 7 plus vector with *tig* or derivatives. Cells were grown at 37°C, and gene expression was induced by addition of AHT (OD_{600} = 0.3; 37°C; 5 ng/ml AHT; 3 h). Equal number of cells (normalized by OD_{600}) was analysed on 12% SDS–PAGE and immune-stained using α-TF. Purified His-TF (20 ng; lane 1) served as a molecular weight/protein amount marker. *n = 3*; a representative experiment is shown.

B Titration of pro-OmpA to define a linear range for ATPase stimulation. pro-OmpA was titrated (0–2 μM; direct dilution from 6 M to 0.12 M urea) into reactions (50 μl; Buffer E) containing SecA (0.4 μM) and SecYEG-IMVs (0.4 μM SecY). The translocation ATPase was measured, and the ratio of translocation over membrane (T/M) ATPase is shown. *n* = 1. Unless otherwise indicated, 0.5 μM pro-OmpA was used for all ATPase experiments (red arrow).

C SecA basal or membrane ATPase activity is not affected neither by SecB nor by TF. The basal (0.4 μM SecA) and membrane (plus SecYEG-IMVs; 0.4 μM SecY) ATPase was measured (50 μl; Buffer E) without or with TF_2, $SecB_4$ or both (as indicated; added at the molar excess over pro-$OmpA_1$ that was used in Fig 1D). *n* = 1–2 biological replicates; mean values ± SEM are shown.

D TF does not affect the translocation of pro-PhoA. pro-$PhoA_1$ (3 μM) was added to reactions [50 μl; Buffer E; SecA (0.4 μM); SecYEG-IMVs (0.4 μMSecY)] that contained, or not (as indicated), TF_2 or $SecB_4$ (at the indicated molar excess over pro-PhoA); as in Panel (B). *n* = 1.

E Equilibrium dissociation constant (K_d) of SecB for SecA bound to SecYEG-IMVs. A concentration range of SecB (0–400 nM) was mixed with SecA (0.4 μM) bound on SecYEG (0.8 μM in 50 μl reactions). Data, analysed by non-linear regression, represent average values; error bars: standard mean error (SEM) is shown; *n* = 6 biological replicates.

F The aggregation propensity of pro-OmpA* under different conditions. pro-OmpA (wild-type; WT) and pro-OmpA* (mutant) pre-treated (10 mM DTT; 5 mM EDTA; 20 min; 4°C) or not were diluted out of chaotrope (Buffer C; < 0.2 M urea) and incubated (60 min; 37°C). Aggregates were removed by centrifugation (20,000 *g*; 10 min; 4°C), and the amount of protein remaining soluble was determined *via* spectroscopic measurements (280 nm; NanoDrop 2000; Thermo). *n* = 6 biological replicates; mean values ± SEM are shown.

Source data are available online for this figure.

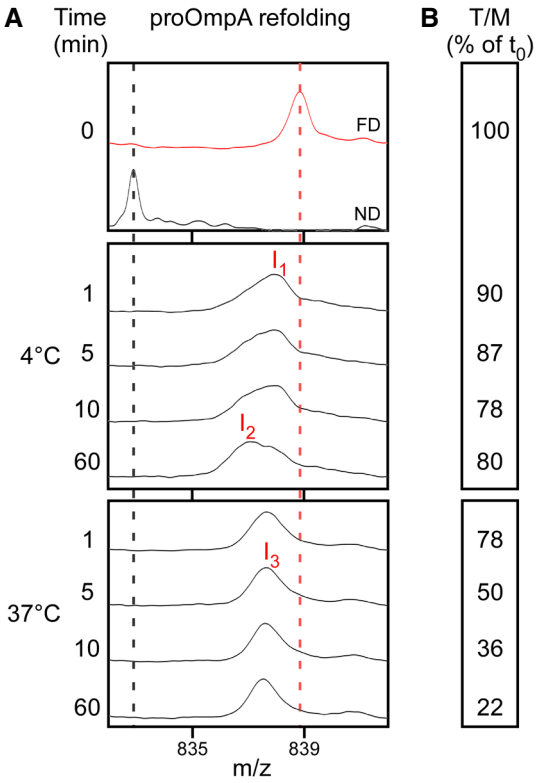

Figure EV2. Time kinetics of pro-OmpA folding at different temperatures, monitored by global HDX-MS analysis and translocation ATPase (related to Figs 2 and 3).

A, B Pre-treated pro-OmpA was diluted from chaotrope into aqueous Buffer D and incubated at the indicated temperature. (A) At the indicated time points, samples were deuterated (100-sec pulse; 4°C or 37°C) quenched on ice (formic acid; pD: 2.1) and analysed by global HDX-MS. Samples were compared to the fully deuterated (FD) and non-deuterated (ND) controls. The (+44) charge state is shown. n = 3. m/z: mass/charge ratio. (B) At the indicated time points, pro-OmpA samples [0.5 μM; for time points 10 and 60 min, a centrifugation step (20,000 g; 10 min; 4°C) has been added] were added to translocation ATPase assays. ATPase activity was measured (as in Fig 1C) and transformed to T/M ratio as in Fig 1D. n = 2. T/M: ratio of translocation and membrane ATPase.

Source data are available online for this figure.

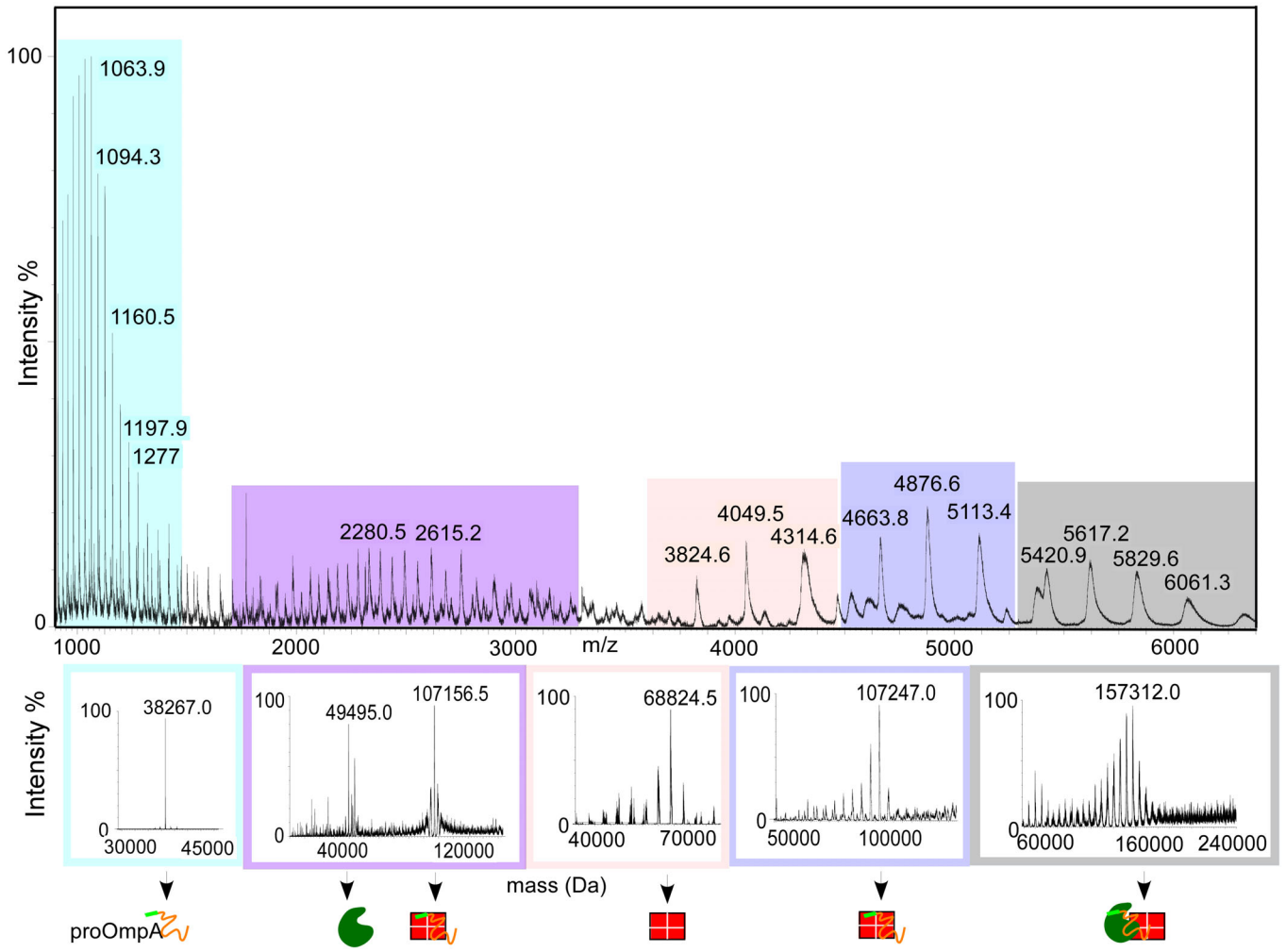

Figure EV3. Native-MS of TF:pro-OmpA:SecB (related to Fig 5).
ESI-mass spectrum and charge state distributions of different populations detected during native-MS analysis of TF:pro-OmpA:SecB complex. pro-OmpA, [TF_1 and ($SecB_4$:pro-OmpA)$_1$], $SecB_4$, ($SecB_4$:pro-OmpA) and the super-complex (TF:pro-OmpA:$SecB_4$)$_1$ are coloured in cyan, violet, light pink, light purple and grey, respectively. The lower panel shows the different populations in mass spectra of the complex deconvoluted to derive the indicated molecular masses.

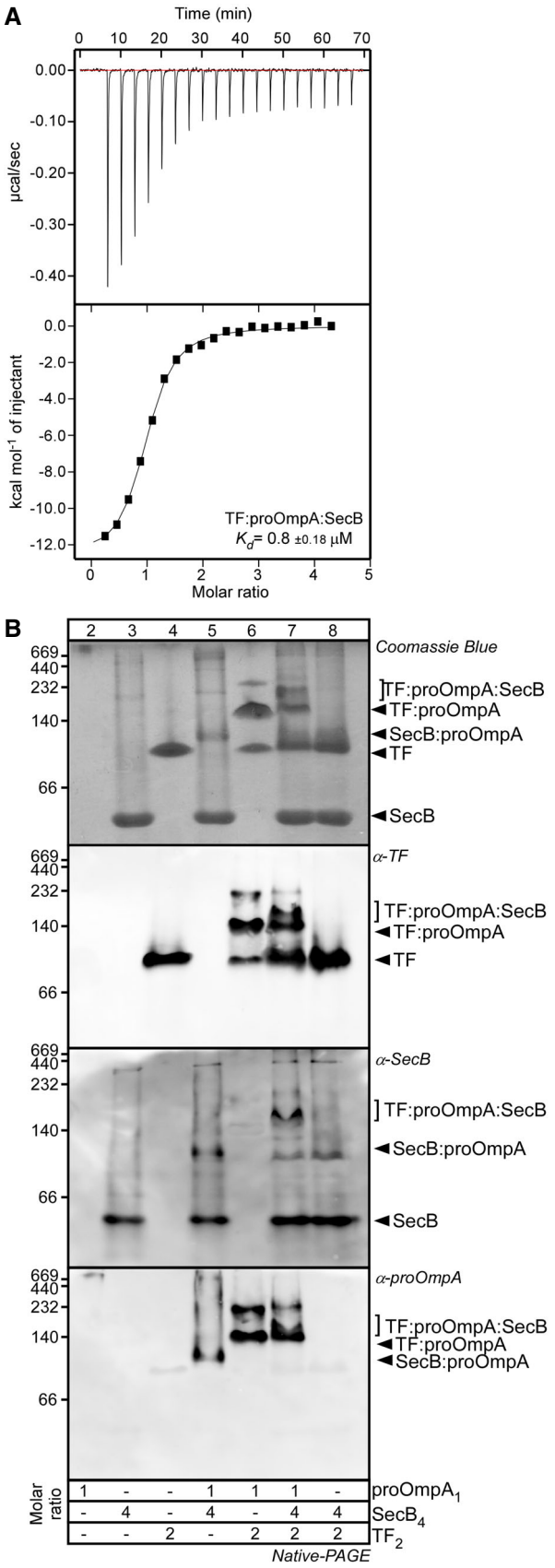

Figure EV4. The TF:pro-OmpA:SecB super-complex analysed by ITC and native-PAGE (related to Fig 5).

A K*d* determination of TF:pro-OmpA:SecB complex in solution by ITC. TF_2:pro-$OmpA_1$ (15 µM; cell) was titrated with $SecB_4$ (128 µM; syringe) in Buffer H at 25°C using an iTC_{200} (Malvern). The injection profile (raw data; top panel) and the calorimetric binding isotherm (bottom panel) are shown. A representative experiment is shown; n = 3.

B Clear native-PAGE analysis of TF:pro-OmpA:SecB complex. The indicated proteins and their complexes were analysed as in Fig 2A. Gels were stained with Coomassie Blue (top) or with the indicated polyclonal antisera. Representative experiments are shown; n = 3 biological repeats.

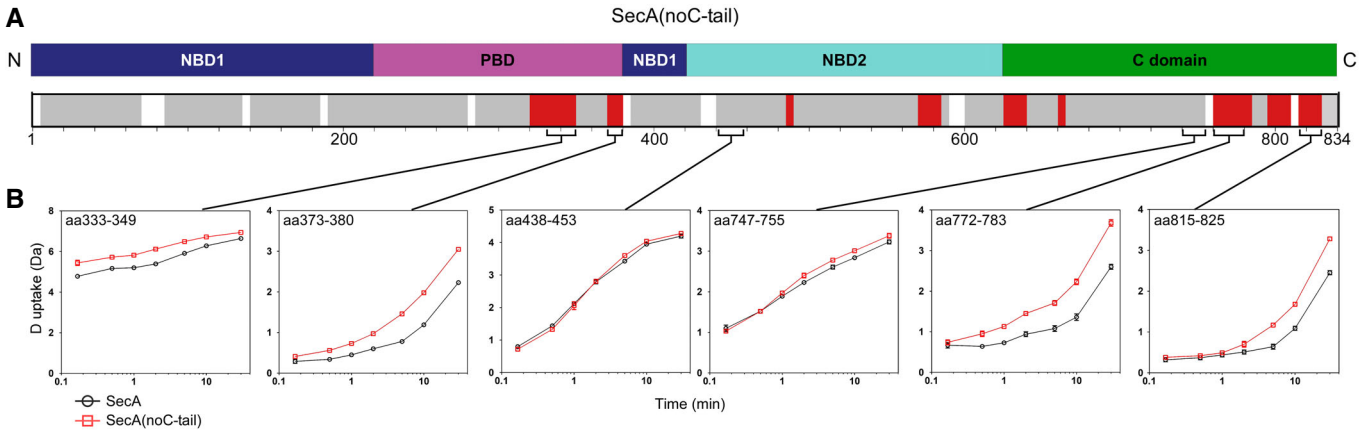

Figure EV5. Local HDX-MS analysis of the SecA(noC-tail) variant (related to Fig 6).

A Linear map of SecA(noC-tail) with the four structural domains indicated the following: nucleotide binding domain 1 (NBD1, dark blue), preprotein binding domain (PBD, magenta), nucleotide binding domain 2 (NBD2, cyan) and C-terminal domain (C domain, green). Local HDX-MS experiments on SecA and SecA(noC-tail) were carried out in identical conditions and directly compared. Removal of the C-tail results in increased dynamics across SecA. Regions with increased dynamics are indicated in red; those that show no differences between SecA and SecA(noC-tail) in grey, regions for which no data are available are in white. $n = 3$.

B Representative D uptake plots for selected peptides from different regions of SecA. D uptake values from SecA (black) and SecA(noC-tail) (red) are plotted with respect to D labelling time. Peptides located mainly in PBD, and the C domain showed increased dynamics in SecA(noC-tail), while most other regions of SecA showed no major differences. Representative experiment is shown; $n = 3$; aa: amino acid.